Available online at www.sciencedirect.com
SCIENCE DIRECT®
International Journal of Heat and Mass Transfer 49 (2006) 52–62
International Journal of HEAT and MASS TRANSFER
www.elsevier.com/locate/ijhmt

Effectiveness of energy wheels from transient measurements. Part I: Prediction of effectiveness and uncertainty

O.O. Abe, C.J. Simonson *, R.W. Besant, W. Shang

Department of Mechanical Engineering, University of Saskatchewan, 57 Campus Drive, Saskatoon, SK, Canada S7N 5A9

Received 15 June 2005; received in revised form 5 August 2005
Available online 13 October 2005

Abstract

An analytical model is presented for predicting the effectiveness of rotating air-to-air energy wheels using only the characteristics measured on the same non-rotating wheels exposed to a step change in temperature and humidity. A relationship between the step change response and the periodic rotating response of an energy wheel is developed assuming that the energy wheel behaves as a first order linear system for water vapour and sensible energy exchange. This allows the prediction of the effectiveness of an energy wheel when only the characteristics of a stationary wheel exposed to humidity and temperature step responses are known. In Part I of this paper, effectiveness correlations and uncertainty bounds are developed for sensible and latent effectiveness of energy wheels using data from transient measurements.

Keywords: Time constant; Transient; Effectiveness; Energy wheel; Linear system model

1. Introduction

Energy wheels are regenerative exchangers used to transfer heat and water vapour between supply and exhaust airstreams in HVAC systems. During hot and humid weather, air flows through the desiccant coated wheel matrix in the supply section and heat and moisture are stored in the supply section of the wheel matrix. As the wheel rotates, the thermal or sensible energy and moisture stored in the supply air section of the wheel matrix during hot humid supply air conditions are released to the dryer and cooler air flowing through the exhaust section. As a result of the wheel rotation, heat and moisture are continuously transferred between the supply and exhaust airstreams as the wheel matrix is exposed to steady periodic changes in input conditions.

Since outdoor and indoor conditions change quite slowly (order of hours) compared to the time constant of energy wheels (e.g. of the order of 10 s [1]), energy wheels operate under essentially steady state conditions. During the steady operation of HVAC systems, energy wheel matrices are dynamic systems with a periodic input and output. Therefore, the hypothesis of this research is that it is possible to predict the steady state response of an energy wheel to a periodic input using only data obtained from a single step change in humidity and temperature. The goal of this research is to develop a relationship between the step (or transient) response and the periodic (or steady state) response of a

* Corresponding author. Tel.: +1 306 966 5479; fax: +1 306 966 5427.
E-mail address: carey.simonson@usask.ca (C.J. Simonson).

0017-9310/$ - see front matter © 2005 Elsevier Ltd. All rights reserved.
doi:10.1016/j.ijheatmasstransfer.2005.08.002

Nomenclature

a	characteristic of the system, inverse of the time constant, τ (s^{-1})
a_n	constant in Fourier series
A'	energy amplitude ratio
A_s	heat and mass transfer surface area on the supply or exhaust side (m^2)
b	constant forcing or input function (K or kg/m^3) or constant in Fourier series
c	constant of integration
C_p	specific heat capacity (J/(kg K))
C_r	ratio of the minimum to maximum heat capacity rate of the air streams
C_r^*	overall heat (or moisture) capacity ratio
d	constant defined in Eq. (41)
e	constant defined in Eq. (41)
f	function of
$f(t)$	forcing function or external input (K or kg/m^3)
$af(t)$	experimental forcing function or external input (K/s or kg/(m^3 s))
h	convective heat transfer coefficient (W/(m^2 K))
h_m	convective mass transfer coefficient (m/s)
L	thickness of wheel (m)
M	total mass of wheel (kg)
$\dot{m}$	mass flow rate of dry air on the supply or exhaust side (kg/s)
N	angular speed of the wheel (cycle/s)
n	integer constant in Fourier series
NTU	number of transfer units
p	period of exposure per cycle for the supply or exhaust gas (s/cycle)
Q	volume flow rate of air on the supply or exhaust side (m^3/s)
RH	relative humidity
rpm	revolutions per minute
t	time (s)
t^*	dimensionless time $\left(\frac{1}{p}\left(t-\frac{z}{\overline{U}}\right)\right)$
T	bulk temperature (°C or K)
u	mass fraction of water in the desiccant (kg_w/kg_d)
$\overline{U}$	mean air flow velocity in an exchanger flow channel (m/s)
$U(\eta)$	uncertainty in parameter η
w	angular frequency of the forcing function (rad/s)
x	output or response of the system, the same as $x(t)$
z	axial coordinate (m)
z^*	dimensionless axial coordinate (z/L)

Greek symbols

α	phase shift angle (rad)
ε	effectiveness
θ	angle of wheel rotation (rad)
ρ	density (kg/m^3)
τ	time constant, wheel alone (s)
χ	weighting factor of a time constant
ψ	dependent variable (temperature, humidity ratio or enthalpy) used in Eq. (1)
$\aleph$	constant defined in Eq. (31)
∞	infinity

Subscripts

a	air
CF	counterflow
d	desiccant
e	exhaust
i	inlet
g	total gas phase (air and water vapour)
m	matrix (including support material, desiccant and moisture)
min	minimum
mt	dimensionless moisture transfer group for energy wheels
o	outlet
PF	parallel flow
s	supply
v	water vapour

Superscript

rec	recuperator

regenerative heat and moisture exchange wheel. Using data from the step (or transient) response, this relationship will then be used to predict the performance or effectiveness of the wheel under periodic (or steady state) operating conditions.

The effectiveness is the prime performance factor to determine the economic viability or feasibility of an energy exchanger for any HVAC application. Since the inlet operating conditions (temperature, humidity, and air flow rate) usually change quite slowly in typical HVAC applications, the effectiveness, determined at steady-state test conditions is used to characterize the performance of energy exchangers. ASHRAE Standard 84–91 [2] uses Eq. (1) to define this steady state effectiveness as

$$\varepsilon = \frac{\dot{m}_s(\psi_i - \psi_o)|_s}{\dot{m}_{min}(\psi_{s,i} - \psi_{e,i})}, \quad (1)$$

where

$$(\psi_i - \psi_o)|_s = (\psi_o - \psi_i)|_e \quad (2)$$

for balanced mass flow and energy rates, (i.e., $\dot{m}_s = \dot{m}_e$). $\dot{m}$ is the mass flow rate of dry air and ψ represents the air temperature, humidity ratio and enthalpy for sensible, latent and total effectiveness, respectively. $\dot{m}_{min}$ is the minimum value of either $\dot{m}_s$ or $\dot{m}_e$. Subscripts i, o, s and e represent the inlet, outlet, supply and exhaust sides of the energy exchanger.

There have been several research papers which have presented experimental methods, effectiveness data and effectiveness correlations for energy wheels under steady state operating conditions [3–9]. However, there are no research papers in the literature on the determination of effectiveness of energy or heat wheels using measured data from non-steady state (i.e., transient) conditions. Part I of this paper, therefore, presents a theoretical model that allows one to predict the effectiveness of an energy wheel using only data obtained during transient measurements. Since it is important to quantify the uncertainty in the predicted effectiveness [5,6], an uncertainty analysis is included which provides the 95% uncertainty bounds in the effectiveness predicted from transient measurements. Part II of this paper [10] will validate the theoretical model developed in Part I using effectiveness data from several wheels measured according to ASHRAE Standard 84–91 [2].

The objectives of Part I of this paper are to: (1) develop the relationship between the step response and a periodic response of an energy wheel so that if one knows the characteristics of a step response then the periodic response can be predicted and (2) predict the steady state sensible, latent and total effectiveness of an energy wheel and the corresponding uncertainties. To achieve these objectives, mathematical models are developed to predict the air properties (T and ρ_v) as the air leaves an energy wheel when there is a step change in the inlet air humidity and temperature. Then these models are used to predict the outlet conditions of an energy wheel when the input properties are changed in a series of step changes which are periodic or steady state as occurs in rotating energy wheel matrices in HVAC applications.

2. Governing equations

The simplified governing equations that govern the transfer and storage of sensible energy on the supply or exhaust side of a counter flow sensible regenerative heat wheel exchanger are presented by [11] assuming that there is negligible conduction in the air and matrix in the axial (flow) direction. The sensible or thermal energy balance equation on the airside describing the balance between advection heat transfer in the air and convective heat transfer between the air (g) and the wheel matrix (m) is

$$\frac{\partial T_g}{\partial z^*} = \mathrm{NTU}(T_m - T_g). \quad (3)$$

The equation describing the balance between thermal energy storage in the wheel matrix and convective heat transfer between the air flowing through the wheel and the matrix is

$$\frac{\partial T_m}{\partial t^*} = \frac{\mathrm{NTU}}{C_r^*}(T_g - T_m). \quad (4)$$

All symbols are defined in the nomenclature and the governing dimensionless groups are defined as

$$\mathrm{NTU} = \frac{hA_s}{(\dot{m}C_p)_g} \quad (5)$$

and

$$C_r^* = \frac{(MC_p)_m N}{(\dot{m}C_p)_g}. \quad (6)$$

Similarly, the mass diffusion equations for water vapour transfer in a regenerative energy wheel are given by [8] as

$$\frac{\partial \rho_v}{\partial z^*} = \mathrm{NTU}_{mt}(\rho_{v,m} - \rho_v) \quad (7)$$

which describes the mass balance in the air and

$$\frac{\partial \rho_{v,m}}{\partial t^*} = \frac{\mathrm{NTU}_{mt}}{C_{r_{mt}}^*}(\rho_v - \rho_{v,m}) \quad (8)$$

which describes the mass balance in the desiccant material in the wheel matrix. The dimensionless groups describing moisture transfer are:

$$\mathrm{NTU}_{mt} = \frac{h_m A_s}{Q}, \quad (9)$$

which is equal to NTU if the Lewis number is unity, and

$$C_{r_{mt}}^* = \left(\frac{\rho_{d,dry} A_{s,d} L}{Qp}\right)\left(\frac{\partial u}{\partial \rho_{v,m}}\right). \quad (10)$$

2.1. Mathematical model

It is noted that Eqs. (4) and (8) are of the mathematical form of a first-order linear system with time as the independent variable. These equations can be represented by a differential equation in the form

$$\frac{dx}{dt} + ax = af(t), \quad (11)$$

where t is the independent variable time, a is a characteristic of the system (whose inverse is the time constant, τ), $f(t)$ is the forcing function or external input, x is the output or response of the system as a function of time. For this research, the forcing function is a step change in temperature (K) or water vapour density (kg/m^3) of

the air and the output is either the matrix temperature, T_m, or the water vapour density in the matrix $\rho_{v,m}$. The dimensionless time introduced in Eqs. (4) and (8) is defined as

$$t^* = \left(\frac{1}{p}\left(t - \frac{z}{\overline{U}}\right)\right). \tag{12}$$

For small dwell times for air flowing through the wheel (or small carry over ratios in the wheel), $z/\overline{U}$ is negligible and Eq. (12) becomes

$$t^* = \frac{t}{p}. \tag{13}$$

For this operating condition, the time response of the outlet air temperature, T_g, and vapour density, ρ_v, must have similar characteristics as that of the matrix—so by measuring the outlet air response we can get the wheel matrix response characteristics. Introducing Eq. (13) into Eqs. (4) and (8), we have

$$\frac{\partial T_m}{\partial t} + \frac{\mathrm{NTU}}{C_r^* p} T_m = \frac{\mathrm{NTU}}{C_r^* p} T_g \tag{14}$$

and

$$\frac{\partial \rho_{v,m}}{\partial t} + \frac{\mathrm{NTU}_{mt}}{C_{r_{mt}}^* p} \rho_{v,m} = \frac{\mathrm{NTU}_{mt}}{C_{r_{mt}}^* p} \rho_v. \tag{15}$$

Equating Eqs. (14) and (15) with the general differential Eq. (11) implies that the characteristic parameter for heat transfer is

$$a = \frac{1}{\tau} = \frac{\mathrm{NTU}}{C_r^* p}, \tag{16a}$$

while the characteristic for mass transfer is

$$a = \frac{1}{\tau} = \frac{\mathrm{NTU}_{mt}}{C_{r_{mt}}^* p}, \tag{16b}$$

where τ is the time constant. The time constant for heat transfer may be different from the time constant for mass transfer and these time constants will be measured separately. Comparing Eqs. (14) and (15) with Eq. (11) also shows that the forcing function, $af(t)$, is the temperature of the inlet air for heat transfer:

$$af(t) = aT_g \tag{17a}$$

and the water vapour density of the inlet air for mass transfer

$$af(t) = a\rho_v. \tag{17b}$$

Therefore, comparing Eq. (11) with Eqs. (4), (8), (14), (15) which relate the properties of the air and matrix, it is seen that the heat and mass transfer equations are coupled, linear first-order differential equations in time. Hence, a model of a linear first-order system is used in the development of the response relationship. It is important to note that, although Eqs. (3)–(15) can be either for a counter flow or parallel flow exchanger, the forcing function (or boundary conditions) typically used in linear system design theory represents a parallel flow arrangement with both the supply and exhaust flow in the same direction. Therefore, the results obtained from this linear model will represent an energy wheel operating in parallel flow. Later the counter flow results will be predicted using these parallel flow results.

2.2. Response to input functions relevant to energy wheel testing

The output or response of a system to various input functions typical of energy wheels is considered in this section. These input functions are constant (or step) and, secondly, rectangular periodic input functions. These are important because the response of the energy wheel to step input functions [1] will be used to estimate the steady state response which is the response to a rectangular periodic input function as the wheel rotates between supply and exhaust airstreams.

2.2.1. Step input function

The step input function is defined by

$$af(t) = \begin{cases} ab & \text{for } t \geqslant 0, \\ 0 & \text{for } t < 0. \end{cases} \tag{18}$$

When $af(t) = 0$, Eq. (11) is said to be homogenous and the general solution of Eq. (11) is given [12] as

$$x(t) = c\mathrm{e}^{-at}, \tag{19}$$

where $x(t)$ is the output or response of the system and c is a constant of integration.

When $af(t) \neq 0$, Eq. (11) is said to be non-homogenous and the general solution is

$$x(t) = \mathrm{e}^{-at} \int_0^t \mathrm{e}^{at} af(t)\,\mathrm{d}t + c\mathrm{e}^{-at}, \tag{20}$$

where c is a constant of integration. Substituting Eq. (18) into Eq. (20), gives

$$x(t) = b + c\mathrm{e}^{-at}. \tag{21}$$

For the case of $x(0) = 0$, $c = -b$. Therefore, $x(t) = b$ is regarded as the equilibrium or steady state solution and $-b\mathrm{e}^{-at}$ is the transient solution. Fig. 1 shows the response of an energy wheel with various time constants to a step input function $ab = 1$. As expected, the response is quicker as the time constant decreases where 63% of the change occurs during one time constant. Two of the time constants shown in Fig. 1 are representative of humidity and temperature sensors described in Part II of this paper [10] (e.g. $\tau = 4$ s) and energy wheels (e.g. $\tau = 10$ s) according to the research of [1].

2.2.2. Rectangular periodic input and output response

The dynamic operation of an energy wheel matrix rotating between two air streams with constant but

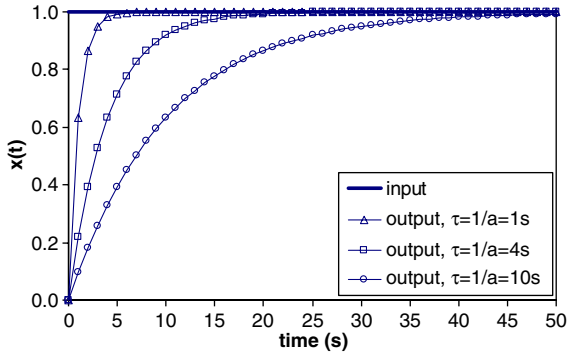

Fig. 1. Step response of a linear system to a unit step input.

different temperature and humidity conditions behaves like a linear system with a steady state rectangular periodic input forcing function. The matrix of an energy wheel rotating between hot and cold air streams will be subject to a step change in the inlet conditions that are periodic, steady and rectangular. The rectangular input function is defined as

$$f(t) = \begin{cases} 1 & \text{for } 0 \leqslant \theta \leqslant \pi, \\ -1 & \text{for } \pi \leqslant \theta \leqslant 2\pi, \end{cases} \tag{22}$$

where θ is the angle of wheel rotation, wt, (radians) and w is the wheel speed (rad/s). This rectangular wave input function can be written in the form of a Fourier series,

$$f(t) = a_{\mathrm{o}} + \sum_{n=1}^{\infty}(a_n \cos nwt + b_1 \sin nwt), \tag{23}$$

where

$$a_0 = \frac{1}{\pi}\int_0^{\pi/w} f(t)\,\mathrm{d}t + \frac{1}{\pi}\int_{\pi/w}^{2\pi/w} f(t)\,\mathrm{d}t = 0, \tag{24}$$

$$a_n = \frac{1}{\pi}\int_0^{\pi/w} f(t)\cos nwt\,\mathrm{d}t + \frac{1}{\pi}\int_{\pi/w}^{2\pi/w} f(t)\cos nwt\,\mathrm{d}t = 0 \quad \text{for all } n \text{ and} \tag{25}$$

$$b_n = \frac{1}{\pi}\int_0^{\pi/w} f(t)\sin nwt\,\mathrm{d}t + \frac{1}{\pi}\int_{\pi/w}^{2\pi/w} f(t)\sin nwt\,\mathrm{d}t = \begin{cases} 4/(n\pi) & \text{for } n = 1,3,5,\ldots \\ 0 & \text{for } n = 2,4,6,\ldots \end{cases} \tag{26}$$

The periodic unit input function $f(t)$ expressed as a Fourier series in Eq. (23) can now be rewritten to get the forcing function $af(t)$

$$af(t) = \frac{4a}{\pi}\sum_{n=1}^{\infty}\frac{\sin nwt}{n} \quad \text{for } n = 1,3,5,\ldots \tag{27}$$

Substituting Eq. (27) as the input forcing function into Eq. (20), the periodic output (or steady-state solution) [13] is

$$x(t) = \sum_{1}^{\infty}\frac{4a}{\pi n(a^2 + (nw)^2)}(a\sin nwt - wn\cos nwt) \quad \text{for } n = 1,3,5,\ldots \tag{28}$$

Rewriting this output response equation using a phase shift angle α, gives

$$x(t) = \sum_{1}^{\infty}\frac{4a}{\pi n\sqrt{a^2 + (nw)^2}}[\sin(nwt - \alpha)] \quad \text{for } n = 1,3,5,\ldots \tag{29}$$

The energy amplitude ratio A', defined as the ratio of the output amplitude to the input amplitude averaged for one half cycle, is a constant when a and w are constant and is given as

$$A' = \sum_{n=1}^{\infty}\frac{a}{\sqrt{a^2 + (nw)^2}} = \sum_{n=1}^{\infty}\aleph_n \quad \text{for } n = 1,3,5,\ldots, \tag{30}$$

where

$$\aleph_n = \frac{a}{\sqrt{a^2 + (nw)^2}} \quad \text{for } n = 1,3,5,\ldots \tag{31}$$

and the corresponding phase shift angle is another constant when a and w are constant

$$\alpha = \tan^{-1}\left(\frac{\left(\sum_{n=1}^{\infty}\frac{4awn}{\pi n\left(a^2 + (nw)^2\right)}\right)^2}{\left(\sum_{n=1}^{\infty}\frac{4a^2}{\pi n(a^2 + (nw)^2)}\right)^2}\right) = \tan^{-1}\left(\sum_{n=1}^{\infty}\frac{nw}{a}\right) \quad \text{for } n = 1,3,5,\ldots \tag{32}$$

Since the magnitude of the terms in the infinite series in Eq. (28) decreases rapidly with increasing n, it is found that including $n \geqslant 21$ is unnecessary in the calculations for the time constants used. Therefore, terms $n \geqslant 21$ are neglected in this paper. The error of neglecting these terms is approximately 0.0001%.

Fig. 2 shows the steady state periodic response $x(t)$ of a system for one cycle with various time constants when the rectangular periodic input function $af(t)$ in Eq. (27) has an angular frequency of (a) $\frac{\pi}{3}$ rad/s (10 rpm) and (b) $\frac{2\pi}{3}$ rad/s (20 rpm). Comparison of Fig. 2(a) and (b) shows that as the wheel speed increases, the amplitude of the system response is reduced. This figure shows the effects of the angular frequency and time constant on the output for a first order linear system. The output of a system with a small time constant follows the input function more closely than a system with a large time constant. In many applications, it is desirable for the output to follow the input closely, but the opposite is

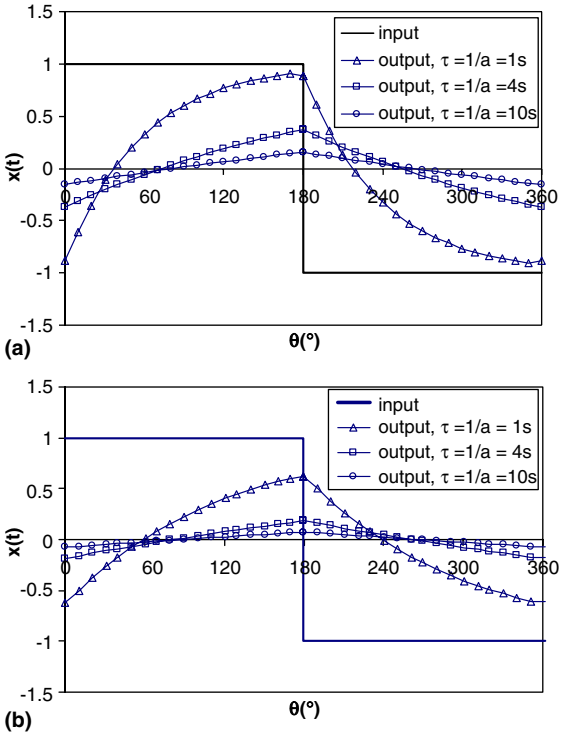

Fig. 2. Periodic response $x(t)$ of a linear system with various time constants for a rectangular steady state periodic input function with (a) $w = \frac{\pi}{3}$ rad/s (10 rpm) and (b) $w = \frac{2\pi}{3}$ rad/s (20 rpm).

the case for a regenerative energy wheel application. The figure also shows that, as the wheel speed increases, the amplitude decreases and the phase shift angle increases.

To help understand this physical process, consider the results in Fig. 2 and imagine that the unit input during the first 180° of rotation represents the inlet hot air stream dimensionless temperature and the input of −1 represents the cold air stream dimensionless temperature. For this example, the output during the first half rotation (0° to 180°) represents the dimensionless temperature of the air leaving the exchanger on the hot side and the output during the second half rotation (180° to 360°) represents the dimensionless temperature of air leaving the exchanger on the cold side. As the wheel rotates from 0° to 180°, the outlet dimensionless temperature on the hot side increases and the exchanger transfers less heat because the wheel temperature approaches that of the flowing air. Since the goal of the exchanger is to cool the hot air stream during the first 180° of rotation (and heat the cold air stream an equal amount during the second 180°), it can be seen that the lower the average output during the first half cycle (and the higher the average output during the second half cycle), the better the exchanger. Therefore the energy amplitude ratio between the output and input is related to the performance of the exchanger such that the lower the energy amplitude ratio, the higher the effectiveness of the exchanger.

3. Effectiveness

The effectiveness of a heat exchanger is defined as the ratio of the actual heat transfer rate to the maximum possible heat transfer rate (for an infinite heat transfer surface area). This same type of definition will be used in this analysis when determining the effectiveness based on the input and output of a linear system. The effectiveness of the system can be defined using the input–output energy ratios. These energy ratios are represented by the areas under the input and the output curves as shown in Fig. 2. Therefore, the effectiveness is defined as the ratio of the *net energy* to the *maximum possible energy* for a parallel flow heat exchanger. The net energy is the difference between the maximum possible (input) area and the output area. The effectiveness for a parallel flow regenerative heat exchanger is thus represented as

$$\varepsilon_{\mathrm{PF}} = \frac{\text{net energy}}{\text{maximum possible energy}}. \tag{33}$$

Since the areas under the output and the input are both symmetrical for a periodic input, as shown in Fig. 2, the average is taken over one-half cycle and Eq. (33) is expressed as

$$\varepsilon_{\mathrm{PF}} = 1 - \frac{w}{2\pi}\int_0^{\pi/w} (1 + x(t))\,\mathrm{d}t, \tag{34}$$

where the output $x(t)$ is given by Eq. (28). After integration, Eq. (34) becomes

$$\varepsilon_{\mathrm{PF}} = 0.5 - \frac{1}{\pi^2}\sum_{n=1}^{\infty} \frac{4a^2}{n^2(a^2 + (nw)^2)} \quad \text{for } n = 1, 3, 5, \ldots \tag{35}$$

It must be noted that though the same formula is used for both sensible and latent effectiveness, they are determined independently. Sensible effectiveness is determined from the transient data obtained when the energy wheel is subjected to a step change in inlet air temperature while the latent effectiveness is determined from the transient data obtained when the energy wheel is subjected to a step change in inlet air relative humidity.

A counter flow heat exchanger has a very high effectiveness when the average outlet temperature of one air stream (say air stream A) is close to the inlet temperature of the other air stream (say air stream B) (and consequently very far from the inlet temperature of air stream A). Therefore it is desired that the output does not rapidly follow the input. A parallel flow exchanger with balanced supply and exhaust air flows will have a maximum effectiveness of 50% when the average outlet

temperatures of both air streams are equal to the average temperature of the two inlet air streams.

The behaviour of the system, expressed as the energy amplitude ratio, is a function of energy transferred [14]. Hence, the effectiveness of the system based on energy can also be defined as a function of the energy amplitude ratio of the system since the energy amplitude ratio is the ratio of the average output amplitude over the cycle to the input amplitude. It follows from Fig. 2 and the previous statements, that an exchanger that operates with balanced supply and exhaust air flows or $C_r = 1$ will have maximum effectiveness (i.e., will approach 50% for parallel flow and 100% for counter flow) as the energy amplitude ratio approaches 0 and the phase lag approaches 90°. Therefore, for an energy exchanger, a lower output amplitude results in a lower energy amplitude ratio and the exchanger effectiveness will be higher. Substituting Eqs. (30) and (31) into Eq. (35) provides the relationship between effectiveness ε_{PF} and the energy amplitude ratio A'. Thus the effectiveness of a parallel flow exchanger (ε_{PF}) can also be expressed as

$$\varepsilon_{PF} = \frac{1}{2}\left[1 - \frac{8}{\pi^2}\sum_{n=1}^{\infty}\left(\frac{\aleph_n}{n}\right)^2\right] \quad \text{for } n = 1, 3, 5, \ldots \tag{36}$$

Fig. 3(a) shows the effectiveness ε_{PF} (defined in Eqs. (35) and (36)) as a function of wheel speed for various time constants ($1/a = \tau$). This figure shows that the effectiveness increases as both the time constant and wheel speed increase. It should be noted that increasing the energy wheel speed to a high value will have another less desirable consequence. It will increase the carry over of exhaust air to the supply side; so manufacturers limit the wheel speed to a practical range (e.g. 20–40 rpm) and the carry over is small fraction of the total air flow rate [6,7]. This leaves the time constant as the main parameter that needs to be examined. As the time constant increases, the output amplitude decreases (as shown in Fig. 2) thereby reducing the energy amplitude ratio. Eq. (36) shows that a reduction in the energy amplitude ratio increases the effectiveness. In Fig. 3(a), the effectiveness increases from 0% to 50% as the wheel speed increases from 0 rpm to 50 rpm for time constants of 4 s and 10 s. At very large wheel speeds, the effectiveness approaches (50%) as expected for a parallel flow heat exchanger (recuperator) with $C_r = 1$. As an example, the effectiveness is 49.9% at 20 rpm when $\tau = 10$ s.

To verify the effectiveness calculated from the linear system model, the results predicted from Eq. (35) are compared with analytical solutions of [15,16] for a parallel flow heat regenerator. Using Eqs. (6) and (16) to relate the key parameter in the linear system model (i.e., τ and w) with the key parameters in the analytical solution of [15] (i.e., NTU and C_r^*) allows a direct comparison between the linear model used in the paper and the analytical solution. Fig. 3(a) shows that the thermal effectiveness values calculated from the linear model (i.e., Eq. (35)) are in very close agreement with the results predicted by [15]. The average and maximum differences between the effectiveness values determined with Eq. (35) and the analytical solution are 0.001 and 0.002, respectively. This demonstrates the accuracy of the linear system model applied in this paper.

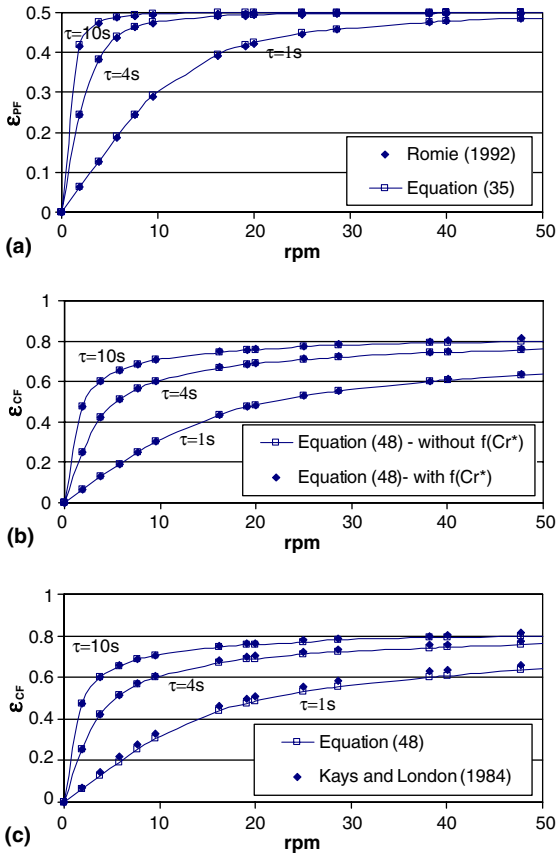

Fig. 3. Comparisons of predicted effectiveness of parallel flow and counter flow energy wheel as a function of the wheel speed for various time constants. (a) Parallel flow, (b) and (c) counter flow.

Since energy exchangers are almost always used in a counter flow and not parallel flow configuration, the effectiveness expression obtained thus far for a parallel flow regenerator (Eq. (35)) will now be related to a counter flow configuration. It is known that the effectiveness of a regenerator (ε) can be calculated as a product of the effectiveness of a recuperator (ε^{rec}) and a constant which is a function of C_r^* [8,9,17]

$$\varepsilon = \varepsilon^{rec} \cdot f(C_r^*), \tag{37}$$

where C_r^* represents the overall matrix heat (or moisture) capacity ratio. Therefore, the effectiveness of a parallel flow (PF) sensible heat regenerator can be calculated as

$$\varepsilon_{PF} = \varepsilon_{PF}^{rec} \cdot f_{PF}(C_r^*), \tag{38}$$

where $f_{PF}(C_r^*)$ means the constant which is a function of C_r^* for an exchanger operating in a parallel flow configuration and ε_{PF}^{rec} is the effectiveness of a parallel flow recuperator. The effectiveness of a parallel flow heat exchanger (recuperator) with $C_r = 1$ is given [18] as

$$\varepsilon_{PF}^{rec} = 0.5(1 - e^{-2NTU_{PF}}). \tag{39}$$

Using Eqs. (35), (38) and (39), an "NTU–a" relationship for parallel flow heat regenerators can be established as

$$NTU_{PF} = -0.5\ln\left(1 - \frac{1}{f_{PF}(C_r^*)} + \sum_{n=1}^{\infty} \frac{8a^2}{f(C_r^*)(\pi n)^2(a^2 + (\pi w)^2)}\right) \quad \text{for } n = 1,3,5,\ldots \tag{40}$$

Note that this equations allows the calculation of NTU from a, w and $f_{PF}(C_r^*)$. Also, as a decreases (i.e., τ increases), NTU increases. To determine $f_{PF}(C_r^*)$ the results of the analytical solution presented by [15] are curve-fitted using a relationship of the same form used for counter flow regenerators [8,9,17], which is

$$\varepsilon_{PF} = \varepsilon_{PF}^{rec}\left[1 - \frac{1}{d(C_r^*)^e}\right], \tag{41}$$

where the values of constants d and e are adjusted to give the best fit. The value of d obtained is 330 and the value of e is 0.47. This makes the second term in Eq. (41) (i.e., the term in the square brackets) to be within the range of

$$0.999 < f_{PF}(C_r^*) < 0.9998 \tag{42}$$

when $C_r^* \geqslant 5$ for typical energy wheel operating condition. Thus the term $f_{PF}(C_r^*)$ can be assumed equal to 1 for practical energy wheels and NTU can be determined knowing only the time constant and the wheel speed.

As previously stated, the aim is to relate the effectiveness of a parallel flow regenerator to a counter flow configuration. The effectiveness for a counter-flow (CF) sensible heat regenerator is presented by [17] as

$$\varepsilon_{CF} = \varepsilon_{CF}^{rec}\left[1 - \frac{1}{9(C_r^*)^{1.93}}\right], \tag{43}$$

where

$$\varepsilon_{CF}^{rec} = f(NTU, C_r). \tag{44}$$

For typical energy wheels, $C_r^* \geqslant 5$ for wheel speed $\geqslant 15$ rpm, giving a practical range for the second term in Eq. (43) as

$$0.995 < f_{CF}(C_r^*) < 0.9998, \tag{45}$$

where $f_{CF}(C_r^*)$ means a function of C_r^* for an exchanger operating in a counter flow configuration. Thus the term $f_{CF}(C_r^*)$ can be assumed equal to 1 for practical energy wheels. Eqs. (42) and (45), which are approximately equal to 1, simplify the relationship between the effectiveness of a sensible heat regenerator operating with a parallel flow configuration and one operating with a counter-flow configuration. For the same mass flow rate of air for both cases, the NTU for the counter flow (CF) regenerator is equal to the NTU for parallel flow regenerator (PF), i.e.,

$$NTU_{CF} = NTU_{PF}. \tag{46}$$

The statement that $NTU_{CF} = NTU_{PF}$ when the mass flow rate and inlet property conditions are the same in counter flow and parallel flow results from the fact that convection heat transfer coefficients between the air and the matrix are the same whether the air flow is arranged in counter flow or parallel flow. Therefore, the effectiveness of a counter-flow heat regenerator with $C_r = 1$ and $f_{CF}(C_r^*) \approx 1$ can be approximated as

$$\varepsilon_{CF} = \varepsilon_{CF}^{rec} = \frac{NTU_{CF}}{1 + NTU_{CF}}. \tag{47}$$

Substituting Eqs. (40) and (46) into Eq. (47), the effectiveness for a counter-flow regenerative heat wheel exchanger with $C_r = 1$ and $f_{CF}(C_r^*) \approx 1$ can be expressed as

$$\varepsilon_{CF} = \frac{-0.5\ln\left[\sum_{n=1}^{\infty} \frac{8a^2}{(\pi n)^2(a^2 + (nw)^2)}\right]}{1 - 0.5\ln\left[\sum_{n=1}^{\infty} \frac{8a^2}{(\pi n)^2(a^2 + (nw)^2)}\right]} \quad \text{for } n = 1,3,5,\ldots \tag{48}$$

Eq. (48), therefore shows that the effectiveness of a regenerative exchanger (i.e., energy wheel) with a counter-flow configuration can be predicted when the time constant of the wheel (which will be determined from the experimental step response in Part II [10]) and the wheel speed are known. The predicted effectiveness of a counter-flow energy wheel with various time constants using Eq. (48) is shown in Fig. 3(b). Note that the effect of assuming $f_{CF}(C_r^*) \approx 1$ on the predicted effectiveness is trivial as shown in Fig. 3(b).At a practical range of 20 to 40 rpm typical of HVAC systems, $f_{CF}(C_r^*)$ does not show much effect on the effectiveness. The maximum difference obtained is 0.02. This figure shows that as the time constant and wheel speed increase, the effectiveness increases. This is as expected because Eq. (40) showed that energy wheels that have larger time constant will have larger values of NTU. The larger the NTU, the larger the heat transfer surface area and thus the higher the effectiveness. To verify the effectiveness calculated from Eq. (48), the results shown in Fig. 3(b) are compared with results obtained from effectiveness correlation of [17] and good agreements are obtained as shown in Fig. 3(c).

In the research of [1] and Part II of this paper[10], it is found that using one time constant did not result in

good correlations for the humidity or temperature step response obtained from experiments; therefore, two-time constant correlations with corresponding weighting factors are used. For combined effects of these time constants and their corresponding weighting factors, NTU_{CF} is defined as

$$NTU_{CF} = \chi_1 NTU_{CF,1} + \chi_2 NTU_{CF,2}, \tag{49}$$

where

$$\chi_1 + \chi_2 = 1, \quad \chi_1 \geqslant 0, \quad \chi_2 \geqslant 0 \tag{50}$$

but with different values of χ_1 and χ_2 for each experiment. χ is the weighting factor of each time constant and subscripts 1 and 2 are for the properties (i.e., χ and NTU_{CF}) of the first and second time constants, respectively. In Part II [10], Eq. (49) will be used in Eq. (47) to determine the effectiveness of energy wheels whose humidity or temperature step response correlation has two time constants and two corresponding weighting factors.

4. Uncertainty in effectiveness

In this section, the uncertainty in the effectiveness predicted with Eq. (48) is determined using 95% confidence limit. This uncertainty in the effectiveness is calculated based on the fact that the uncertainty in the measured time constant, $\tau = 1/a$ can be determined from experiments (see Part II [10]). Knowing the uncertainty in the time constant ($U(\tau)/\tau = U(a)/a$), the uncertainty in the effectiveness can be determined. The uncertainty in the effectiveness of an energy wheel with counter flow configuration is calculated using

$$U(\varepsilon_{CF}) = \left[\left(\frac{\partial \varepsilon_{CF}}{\partial a} U(a)\right)^2\right]^{1/2}. \tag{51}$$

Using Eq. (49),

$$\frac{\partial \varepsilon_{CF}}{\partial a} = \sum_{n=1}^{\infty}\left[\frac{-8aw^2}{\pi^2(a^2+(nw)^2)^2(e^{-2NTU})(1+NTU)^2}\right] \times [1+2NTU] \quad \text{for } n = 1,3,5,\ldots \tag{52}$$

and the uncertainty in the effectiveness of the counter flow regenerator is

$$U(\varepsilon_{CF}) = \left[\left\{\sum_{n=1}^{\infty}\left[\frac{-8aw^2}{\pi^2(a^2+(nw)^2)^2(e^{-2NTU})(1+NTU)^2}\right] \times [1+2NTU](U(a))\right\}^2\right]^{1/2} \quad \text{for } n = 1,3,5,\ldots \tag{53}$$

5. Sensitivity studies

Assuming uncertainty limits for the measured time constants ($U(\tau)/\tau = U(a)/a = \pm 10\%$ or $\pm 15\%$, the sensitivity of the uncertainty in effectiveness to the uncertainty in the measured time constant and the magnitude of the time constant can be determined with Eq. (53). In addition, the sensitivity of the effectiveness and the uncertainty in effectiveness to the wheel speed can be demonstrated.

In Fig. 4(a), the effect of various uncertainty limits in the measured time constant on the uncertainty in the predicted effectiveness is shown. It should be noted that the typical uncertainties in the time constants measured using the newly designed transient response device for energy wheels is ($U(\tau)/\tau = U(a)/a = \pm 10\%$ to $\pm 15\%$ ([1] and Part II [10]). It is seen from Fig. 4(a) that as the uncertainty in the measured time constant increases, the uncertainty in effectiveness increases for all time constants. In addition, at any typical value of the uncertainty in the measured time constant, the uncertainty in effectiveness decreases as the time constant increases. Fig. 4(a) shows that for a time constant of 10 s and an uncertainty of $U(\tau)/\tau = \pm 10\%$ and $\pm 15\%$, the uncertainty in effectiveness $U(\varepsilon_{CF}) = \pm 4.2\%$ and $\pm 6.4\%$, respectively.

In Fig. 4(b), the effect of various time constants on the uncertainty in the predicted effectiveness is shown. This figure shows the predicted uncertainty in the effectiveness of the wheel as a function of the time constant for $U(\tau)/\tau = U(a)/a = \pm 10\%$. As the time

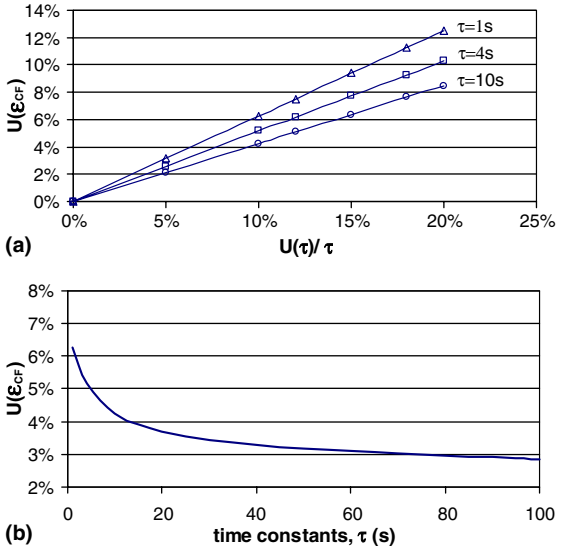

Fig. 4. The sensitivity of uncertainty in effectiveness to (a) the uncertainty in the measured time constant and (b) the value of the time constant when $U(\tau)/\tau = \pm 10\%$. Both graphs are for a wheel speed of 20 rpm.

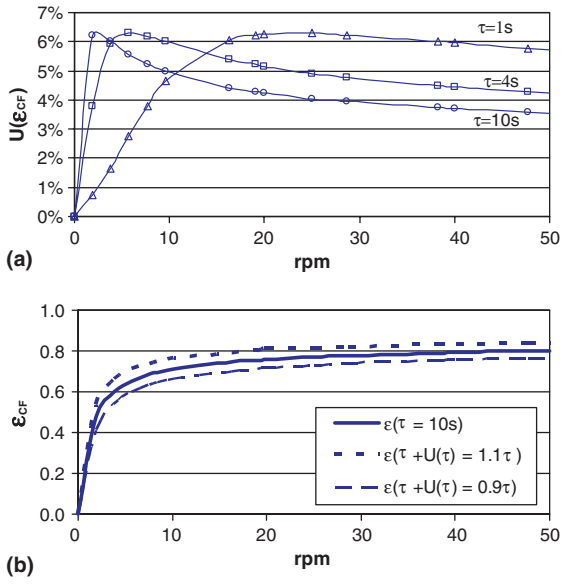

Fig. 5. Sensitivity of (a) uncertainty in effectiveness and (b) effectiveness to wheel speed for $U(\tau)/\tau = \pm 10\%$.

constant increases, the predicted uncertainty limits in ε_{CF} decrease. The figure shows that for an uncertainty limit of $\pm 10\%$ in the time constant, the uncertainty in effectiveness can be predicted within $\pm 3\%$ to $\pm 5\%$ for time constants of about 5–40 s, which is expected to be the case for most commercial wheels (Part II [10]).

The sensitivity of the uncertainty in effectiveness (assuming an uncertainty in the time constant of $U(\tau)/\tau = \pm 10\%$) to the wheel speed is shown in Fig. 5(a). This figure shows that the uncertainty in effectiveness for all time constants is zero at a wheel speed of 0 rpm. As the wheel speed increases from zero to larger values, the uncertainty in effectiveness increases to about 6% and then decreases as the wheel speed becomes very large.

Both the predicted effectiveness and the uncertainty in the effectiveness depend on the wheel speed. To show this effect more clearly, the effectiveness and uncertainty in effectiveness for a time constant of 10 s having an uncertainty of $U(\tau)/\tau = \pm 10\%$ is shown in Fig. 5(b). The figure shows that at a typical operating wheel speed of 20 rpm, the effectiveness $\varepsilon_{CF} = 76\%$ and the uncertainty in the effectiveness $U(\varepsilon_{CF}) = \pm 4.2\%$ while at a wheel speed of 40 rpm, the effectiveness $\varepsilon_{CF} = 79\%$ and the uncertainty in effectiveness $U(\varepsilon_{CF}) = \pm 3.7\%$. This shows that the effectiveness increases as the wheel speed increases and the uncertainty in effectiveness decreases as the wheel speed increases. Using the method in this paper, a manufacturer could simply and easily choose the optimal wheel speed for maximum effectiveness without resulting in excessive carry-over of exhaust air into the supply air stream at design conditions. During other operating conditions, the wheel speed could be controlled to optimize the performance of the system.

6. Conclusions

In this paper, an analytical model is developed to predict the effectiveness and uncertainty in effectiveness of a counter flow energy wheel knowing the time constant of the wheel and uncertainty in the time constant. This model shows that (a) the effectiveness increases as the time constant and wheel speed increase, and (b) the uncertainty in the effectiveness decreases as the wheel speed and time constant increase. Using this method, the effectiveness of energy wheels can be predicted with uncertainties of $\pm 3\%$ to $\pm 5\%$.

Acknowledgements

Financial assistance from the Natural Sciences and Engineering Research Council of Canada (NSERC) and Venmar CES, Saskatoon is appreciated.

References

[1] Y.H. Wang, C.J. Simonson, R.W. Besant, W. Shang, Transient humidity measurements and characteristics for humidity sensors and energy wheels, ASHRAE Trans. 111 (2) (2005) 353–369.
[2] ASHRAE Standard 84-1991, Method of testing air-to-air heat exchangers, American Society of Heating, Refrigerating and Air Conditioning Engineers Inc., Atlanta, 1991.
[3] H.N. Gawley, D.R. Fisher, The effectiveness and rating of air-to-air heat exchangers, ASHRAE Trans. 81 (2) (1975) 401–409.
[4] H. Klein, S.A. Klein, J.W. Mitchell, Analysis of regenerative enthalpy exchangers, Int. J. Heat Mass Transfer 33 (1990) 735–744.
[5] D.L. Ciepliski, C.J. Simonson, R.W. Besant, Some recommendations for improvements to ASHRAE Standard 84–91, ASHRAE Trans. 104 (1B) (1998) 1651–1965.
[6] C.J. Simonson, D.L. Ciepliski, R.W. Besant, Determining the performance of energy wheels: Part I—experimental and numerical methods, ASHRAE Trans. 105 (1) (1999) 188–205.
[7] C.J. Simonson, D.L. Ciepliski, R.W. Besant, Determining the performance of energy wheels: Part II—experimental data and numerical validation, ASHRAE Trans. 105 (1) (1999) 177–187.
[8] C.J. Simonson, R.W. Besant, Energy wheel effectiveness: Part I—development of dimensionless groups, Int. J. Heat Mass Transfer 42 (1999) 2161–2170.
[9] C.J. Simonson, R.W. Besant, Energy wheel effectiveness: Part II—correlations, Int. J. Heat Mass Transfer 42 (1999) 2171–2185.

[10] O.O. Abe, C.J. Simonson, R.W. Besant, W. Shang, Effectiveness of energy wheels from transient measurements: Part II—Results and verification, Int. J. Heat Mass Transfer, in press, doi:10.1016/j.ijheatmasstransfer.2005. 08.009.
[11] R.K. Shah, Thermal design theory for regenerators, in: S. Kakaç, A.E. Bergles, F. Mayinger (Eds.), Heat Exchangers: Thermal–Hydraulic Fundamentals and Design, Hemishere, New York, 1981, pp. 721–763.
[12] W. Kaplan, Advanced Mathematics for Engineers, Addison-Wesley, Ontario, 1981, pp. 20–22.
[13] E. Kreyszig, Advanced Engineering Mathematics, Wiley, New York, 1999, pp. 526–581.
[14] I. Cochin, H.D. Plass Jr., Analysis and Design of Dynamic Systems, HarperCollins, New York, 1990, pp. 181–184.
[15] F.E. Romie, A solution for the parallel flow regenerator, J. Heat Transfer 114 (1992) 278–280.
[16] H. Hausen, Heat Transfer in Counter Flow Parallel Flow and Cross Flow, McGraw-Hill, New York, 1983.
[17] W.M. Kays, A.L. London, Compact Heat Exchangers, McGraw-Hill, New York, 1984, pp. 32–33.
[18] F.P. Incropera, D.P. Dewitt, Fundamentals of Heat and Mass Transfer, Wiley, New York, 2002, pp. 659–665.